

# Continuum modelling of spherical and spheroidal carbon onions

D. Baowan<sup>a</sup>, N. Thamwattana, and J.M. Hill

Nanomechanics Group, School of Mathematics and Applied Statistics, University of Wollongong,  
Wollongong, NSW 2522, Australia

Received 23 January 2007 / Received in final form 12 April 2007

Published online 16 May 2007 – © EDP Sciences, Società Italiana di Fisica, Springer-Verlag 2007

**Abstract.** Carbon nanostructures are of considerable interest owing to their unique mechanical and electronic properties. Experimentally, a wide variety of different shapes are obtained, including both spherical and spheroidal carbon onions. A spheroid is an ellipsoid with two major axes equal and the term onion refers to a multi-layered composite structure. Assuming structures of either concentric spherical or ellipsoidal fullerenes comprising  $n$  layers, this paper examines the interaction energy between adjacent shells for both spherical and spheroidal carbon onions. The Lennard-Jones potential together with the continuum approximation is employed to determine the equilibrium spacing between two adjacent shells. We also determine analytical formulae for the potential energy which may be expressed either in terms of hypergeometric or Legendre functions. We find that the equilibrium spacing between shells decreases for shells further out from the inner core owing to the decreasing curvature of the outer shells of a concentric structure.

**PACS.** 02.30.Rz Integral equations – 34.20.-b Interatomic and intermolecular potentials and forces, potential energy surfaces for collisions – 62.25.+g Mechanical properties of nanoscale materials

## 1 Introduction

Carbon nanostructures including fullerenes, carbon nanotubes, nanocones, nanopeapods, nanotorii and carbon onions have received much attention because of their unique properties, such as their high flexibility, their high thermal conductivity and they are presently the strongest material known [1]. We refer the reader to [2, 3] for comprehensive pictorial catalogues of the many diverse structures which may arise. Their special properties have not only led to proposals for many potential nano-devices [4–6] but also to the desire to create further new carbon nanostructures and the spherical and ellipsoidal carbon onions are examples of such structures. Carbon onions comprise multi-layer composite structures and here we consider those of both spherical and spheroidal shapes, noting that a spheroid is simply an ellipsoid with two major axes of equal length. Experimentally, electron beam irradiation methods are used to modify the multi-layers of carbon onions, but at present there are no procedures to predict the precise shape of the resulting structures. The major issue in this regard is the determination of the interspacing layer of such structures. Recently, molecular dynamics simulation techniques have been used to examine the formation of such nanostructures. This calculation may be effected using density functional theory and a tight binding method such as that described in [7] and [8] respec-

tively. However, in this paper rather than undertake such large scale calculations, we employ elementary mechanical principles and classical mathematical modelling to investigate the interaction energies between adjacent shells of spherical and spheroidal carbon onions, which leads to the determination of the equilibrium spacings of such structures.

While there are a number of studies on spherical carbon onions [9–11], very little work has been undertaken for other forms of carbon onions. Kitahara et al. [12] employ an electron beam irradiation technique to experimentally create ellipsoidal carbon onions and they also investigate the stability of these structures by using molecular mechanics and molecular orbital calculations. Narita et al. [13] also utilize electron beam irradiation methods to produce tetrahedral carbon onions, and they determine the energy levels and the density of different states for such tetrahedral carbon onions.

For spherical and spheroidal carbon onions, this paper utilizes the Lennard-Jones potential together with the continuum approximation to determine the potential energy between two adjacent layers. The continuum approximation assumes that the carbon atoms are uniformly distributed over the surface of each molecule, with a constant atomic surface density determined simply by dividing the number of atoms by the surface area of the molecule. From the minimisation of the energy of the structure, this method can be used to predict the spacings between adjacent layers and therefore the lateral and vertical

---

<sup>a</sup> e-mail: db898@uow.edu.au

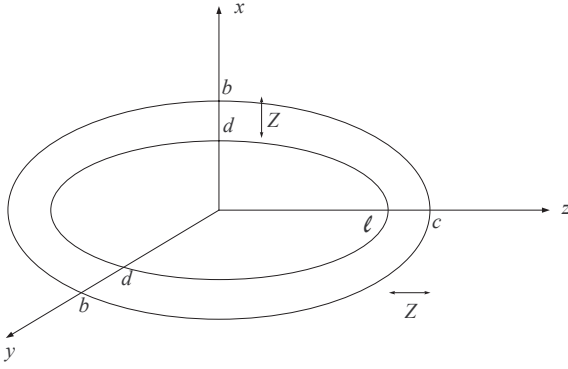


Fig. 1. Double-shell ellipsoidal carbon onion.

dimensions for each layer of spherical and ellipsoidal carbon onions. From curve fitting, we obtain an expression for the equilibrium spacing for any two neighbouring layers of the carbon onions.

## 2 Interaction energies between shells

Here, we consider the interaction energy between two adjacent shells of an ellipsoidal (or spherical) carbon onion. We assume that the ellipsoidal carbon onion comprises a family of concentric nested spheroidal fullerenes located coaxially as shown in Figure 1, noting again that a spheroid, which is also known as an ellipsoid of revolution, is an ellipsoid with two of its radii of equal length.

From Figure 1, with reference to the rectangular Cartesian coordinate system, the parametric equations for the outer and inner spheroids are given by  $(x_1, y_1, z_1) = (b \sin \phi_1 \cos \theta_1, b \sin \phi_1 \sin \theta_1, c \cos \phi_1)$  and  $(x_2, y_2, z_2) = (d \sin \phi_2 \cos \theta_2, d \sin \phi_2 \sin \theta_2, l \cos \phi_2)$ , respectively, where  $\theta_1, \theta_2 \in [0, 2\pi]$  and  $\phi_1, \phi_2 \in [0, \pi]$ . If we assume that the interspacing along the three coordinate axes between two neighbouring shells of the carbon onion is given by  $Z$ , then we have  $l = c - Z$  and  $d = b - Z$ . The distance  $\rho$  between two typical surface elements on the inner and the outer spheroids is given by

$$\begin{aligned} \rho^2 &= (b \sin \phi_1 \cos \theta_1 - d \sin \phi_2 \cos \theta_2)^2 \\ &\quad + (b \sin \phi_1 \sin \theta_1 - d \sin \phi_2 \sin \theta_2)^2 \\ &\quad + (c \cos \phi_1 - l \cos \phi_2)^2 \\ &= (b \sin \phi_1 - d \sin \phi_2)^2 \\ &\quad + 4bd \sin \phi_1 \sin \phi_2 \sin^2[(\theta_1 - \theta_2)/2] \\ &\quad + (c \cos \phi_1 - l \cos \phi_2)^2. \end{aligned}$$

For the continuum approach, we assume that the atoms are uniformly distributed over the surface of the molecule, and we use a constant average atomic density which is simply the number of atoms divided by the surface area of the molecule. Thus, the total potential energy  $E$  for the two molecules can be obtained by performing the surface integrals of a potential function over the two molecules, namely

$$E = \eta_1 \eta_2 \iint V(\rho) dS_1 dS_2, \quad (2.1)$$

where  $\eta_1$  and  $\eta_2$  denote the mean surface densities of the outer and inner ellipsoidal fullerenes and  $\rho$  is the distance between the two surface elements  $dS_1$  and  $dS_2$  on the outer and inner spheroidal fullerenes, which are given respectively by

$$\begin{aligned} dS_1 &= b \sin \phi_1 \sqrt{b^2 \cos^2 \phi_1 + c^2 \sin^2 \phi_1} d\theta_1 d\phi_1, \\ dS_2 &= d \sin \phi_2 \sqrt{d^2 \cos^2 \phi_2 + l^2 \sin^2 \phi_2} d\theta_2 d\phi_2, \end{aligned}$$

and the integration is performed over the entire surface of the two ellipsoids. Further,  $V(\rho)$  denotes the interatomic interaction potential for two typical single atoms located one on each ellipsoid and here we adopt the classical six-twelve Lennard-Jones potential, so that the interaction energy (2.1) between shells of the ellipsoidal carbon onion takes the form

$$E = \eta_1 \eta_2 \int_0^\pi \int_0^\pi \int_0^{2\pi} \int_0^{2\pi} \gamma \left( -\frac{A}{\rho^6} + \frac{B}{\rho^{12}} \right) d\theta_1 d\theta_2 d\phi_1 d\phi_2,$$

and

$$\begin{aligned} \gamma &= bd \sin \phi_1 \sin \phi_2 \\ &\quad \times \sqrt{(b^2 \cos^2 \phi_1 + c^2 \sin^2 \phi_1)(d^2 \cos^2 \phi_2 + l^2 \sin^2 \phi_2)}. \end{aligned}$$

Further, we define the integrals  $I_n^*$  as

$$\begin{aligned} I_n^* &= \int_0^{2\pi} \int_0^{2\pi} \frac{d\theta_1 d\theta_2}{\rho^n} \\ &= \int_0^{2\pi} \int_0^{2\pi} \frac{d\theta_1 d\theta_2}{\{\lambda + \xi \sin^2[(\theta_1 - \theta_2)/2]\}^{n/2}}, \quad (2.2) \end{aligned}$$

where  $n = 6$  and  $12$ ,  $\lambda = (b \sin \phi_1 - d \sin \phi_2)^2 + (c \cos \phi_1 - l \cos \phi_2)^2$  and  $\xi = 4bd \sin \phi_1 \sin \phi_2$ . We note that none of the terms in  $\gamma$ ,  $\lambda$  and  $\xi$  depend on  $\theta_1$  or  $\theta_2$ . In Appendix A, we show that the integrals  $I_n^*$  can be evaluated either in terms of hypergeometric functions or Legendre functions. In terms of the hypergeometric function, we may deduce

$$\begin{aligned} I_6^* &= \frac{4\pi^2}{(\lambda + \xi)^3} F\left(3, \frac{1}{2}; 1; \kappa\right), \\ I_{12}^* &= \frac{4\pi^2}{(\lambda + \xi)^6} F\left(6, \frac{1}{2}; 1; \kappa\right), \quad (2.3) \end{aligned}$$

where  $\kappa = \xi/(\lambda + \xi)$ . Since these equations are degenerate hypergeometric functions (see Appendix B), they can be written as

$$\begin{aligned} I_6^* &= \frac{4\pi^2}{\lambda^2 \sqrt{\lambda(\lambda + \xi)}} \left(1 - \kappa + \frac{3}{8} \kappa^2\right), \\ I_{12}^* &= \frac{4\pi^2}{\lambda^5 \sqrt{\lambda(\lambda + \xi)}} \left(1 - \frac{5}{2} \kappa + \frac{15}{4} \kappa^2 - \frac{25}{8} \kappa^3 \right. \\ &\quad \left. + \frac{175}{128} \kappa^4 - \frac{63}{256} \kappa^5\right). \end{aligned}$$

Thus, the total potential energy becomes

$$E = \eta_1 \eta_2 \int_0^\pi \int_0^\pi \gamma (-AI_6^* + BI_{12}^*) d\phi_1 d\phi_2. \quad (2.4)$$

**Table 1.** Radius of each shell for a spherical carbon onion predicted from minimisation of energy  $E_o/(\eta_1\eta_2)$  (2.5) and assuming a  $C_{60}$  core.

$n$ th-shell	$C_{60}$	2nd	3rd	4th
Radius (Å)	3.55	7.042	10.516	13.981
$n$ th-shell	5th	6th	7th	8th
Radius (Å)	17.442	20.900	24.356	27.811

We note that to obtain the final result for  $E$ , we need to integrate (2.4) with respect to  $\phi_1$  and  $\phi_2$ , and we perform these integrals numerically. Although clearly complicated, numerical values for these integrals can be readily evaluated using the algebraic computer package MAPLE.

For the special case of the spherical carbon onion for which all three major axes are equal, we have from Figure 1 that  $d = \ell$  for the core and  $b = c$  for the outer shell. In this case, the interaction energy between shells can be obtained explicitly, and is given by

$$E_o = -P_6 + P_{12}, \quad (2.5)$$

where  $P_n$  ( $n = 6, 12$ ) are defined by

$$P_n = \frac{8\pi^2 bd C_n \eta_1 \eta_2}{(2-n)} \left( \frac{1}{(b+d)^{n-2}} - \frac{1}{(b-d)^{n-2}} \right), \quad (2.6)$$

where  $C_6 = A$ ,  $C_{12} = B$  and again  $\eta_1$  and  $\eta_2$  represent the surface densities of carbon atoms on the outer and inner spherical fullerenes respectively. We refer the reader to Iglesias-Groth et al. [14] for the derivation of (2.6).

### 3 Numerical results

Here we use the algebraic computer package MAPLE to show graphically the relation between the potential energy and the interspacing between two neighbouring shells for spherical and ellipsoidal carbon onions. The attractive and repulsive constants  $A$  and  $B$  for graphitic carbon interactions are taken to be  $A = 17.4 \text{ eV } \text{Å}^6$  and  $B = 29 \times 10^3 \text{ eV } \text{Å}^{12}$  [15]. Due to the short range interaction of the van der Waals force, we assume that we need only taking into account the interactions between adjacent layers for the calculation of the resultant potential energy [16].

For the spherical carbon onion, we assume that the 1st-shell, or the core, is the spherical  $C_{60}$  fullerene, which has a radius of 3.55 Å. This is consistent with experimental results, where the core of a fully formed spherical carbon onion has the diameter of 7–10 Å [17]. From (2.5) upon substituting  $d = 3.55$ , we may determine  $b$  or the radius of the 2nd-shell, which is the critical value for which the energy  $E_o/(\eta_1\eta_2)$  is minimum. Repeatedly, by using the radius of the  $(n-1)$ th-shell as the value

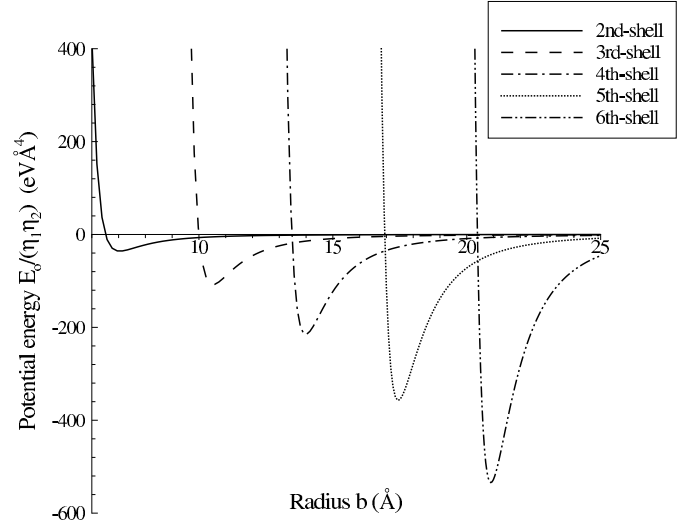


**Fig. 2.** Potential energy profile for a spherical carbon onion showing the possible radii of the  $n$ th-shell for which the energy is minimum.

**Table 2.** Radii of spherical fullerenes  $C_N$ .

Fullerene	$C_{240}$	$C_{540}$	$C_{960}$	$C_{1500}$
Radius (Å)	7.06	10.53	14.02	17.5225
Fullerene	$C_{2160}$	$C_{2940}$	$C_{3840}$	
Radius (Å)	20.95	23.8728	27.95	

of  $d$  in (2.5), we may determine the radius of the  $n$ th-shell,  $b$ , by minimizing  $E_o/(\eta_1\eta_2)$ . Following this procedure, we obtain the radius for each shell of an eight-layer spherical carbon onion, as shown in Table 1. These values are the critical radii shown in Figure 2 for each shell. We comment that the spherical carbon onion comprising shells with radii shown in Table 1 are approximately the structure proposed by Kroto and McKay [18] which is the  $C_{60}@C_{240}@C_{540}@C_{960}@C_{1500}@...@C_N$  spherical carbon onion, where  $N$  is the number of carbon atoms in Goldberg fullerenes of  $I_h$  symmetry type I given by  $N = 60n^2$ , where  $n$  is an integer [1]. We refer to Table 2 for average radii of  $C_N$ , which are taken from Itoh et al. [19] for  $C_{240}$ ,  $C_{540}$ ,  $C_{960}$ ,  $C_{2160}$  and  $C_{3840}$  and from Dunlap and Zope [20] for  $C_{1500}$ . For Goldberg fullerenes of  $I_h$  symmetry type I, the average radius is approximated by  $\bar{R} \approx 2.4\bar{\sigma}n$ , where  $\bar{\sigma}$  is the average bond length [9]. Using  $\bar{\sigma} = 1.421 \text{ Å}$  and  $n = 7$ , we obtain the average radius of  $C_{2940}$  as shown in Table 2.

For spheroidal carbon onions, we consider two cases using  $C_{24}$  [11] and  $C_{80}$  [12] as the core. From (2.4) with the substitutions of  $c = \ell + Z$  and  $b = d + Z$ , the equilibrium distance  $Z$  between two adjacent layers may be obtained from the minimisation of the energy  $E/(\eta_1\eta_2)$ . Using a  $C_{80}$  ellipsoidal fullerene which has a lateral size  $\ell = 4.73 \text{ Å}$  and a vertical size  $d = 3.58 \text{ Å}$  [11] as the

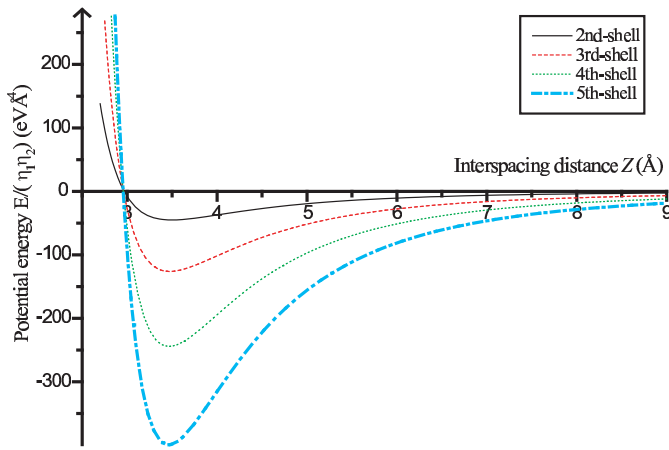


**Fig. 3.** (Color online) Potential energy profile for a five-shell  $C_{80}$  carbon onion.

**Table 3.** Lateral and vertical sizes for five-layer ellipsoidal carbon onion where  $C_{80}$  is assumed inner core.

$n$ th-shell	$C_{80}$	2nd	3rd	4th	5th
lateral radius (Å)	4.73	8.222	11.699	15.167	18.629
vertical radius (Å)	3.58	7.072	10.549	14.017	17.479
mean radius (Å)	4.155	7.647	11.124	14.542	18.054

**Table 4.** Lateral and vertical sizes for five-layer ellipsoidal carbon onion where  $C_{24}$  is assumed inner core.

$n$ th-shell	$C_{24}$	2nd	3rd	4th	5th
lateral radius (Å)	2.315	5.846	9.324	12.792	16.256
vertical radius (Å)	1.665	5.196	8.674	12.142	15.606

inner core, or the 1st-shell, we may determine from (2.4) the equilibrium distance  $Z_{12}$  which is the critical value shown in Figure 3 (—) that minimises the interaction energy between the 1st- and 2nd-shells. Knowing  $Z_{12}$  gives rise to the lateral and vertical sizes of the 2nd-shell, which then become  $\ell$  and  $d$  in the determination of  $Z_{23}$ . Repeatedly, we can determine the equilibrium spacing  $Z_{(n-1)n}$  for the  $(n-1)$ th- and  $n$ th-shells interaction and Figure 3 shows the relation between the energy  $E/(\eta_1\eta_2)$  and the interspacing between two neighbouring shells for the ellipsoidal carbon onion with  $C_{80}$  as the core. The critical values that minimise the potential energy are the equilibrium distance between each layer of the ellipsoidal carbon onion. The lateral and vertical sizes for a five-shell ellipsoidal carbon onion with  $C_{80}$  core are given in Table 3. Using a similar procedure to that described above, we may obtain Table 4, which gives the dimensions of the outer shells for the ellipsoidal carbon onion, where  $C_{24}$  is the core. For the ellipsoidal carbon onions with a  $C_{80}$  core, we note that the equilibrium interlayer spacing between neighbouring shells is approximately 3.4 Å. Further, we find from Terrones et al. [21]

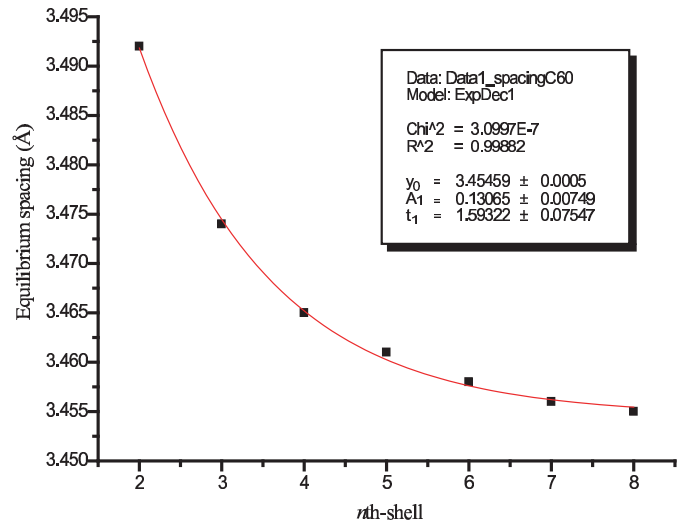


**Fig. 4.** Equilibrium spacing between adjacent shells of spherical carbon onion assuming  $C_{60}$  core.

that the mean radii of  $C_{260}$ ,  $C_{560}$  and  $C_{980}$  are 7.662, 11.057 and 14.588 Å, respectively. As a result, we find from Table 3 that assuming  $C_{80}$  as a core gives rise to the carbon onion structure  $C_{80}@C_{260}@C_{560}@C_{980}@C_{1520}\dots@C_N$  where  $N = 20(m^2 + mn + n^2)$ . As such, our study confirms the possible creation of the nested chiral icosahedral fullerenes of type I symmetry as proposed by Terrones et al. [21].

From the tables, the values of the equilibrium spacing  $Z$  between two adjacent layers for both spherical and ellipsoidal carbon onions decrease the further away the shell is from the inner core, which results from the effect of decreasing curvature of the spheroids. The high curvature of the inner shells means that for any atom on the surface, there can be more than one interacting atom on the neighbouring shell. Moreover, the shells which are further away from the inner core become more like a flat surface, for which the interaction energy of the neighbouring shells is approximately the equilibrium spacing of two graphite sheets. The equilibrium spacing between two adjacent layers is obtained approximately as 3.4 Å for both cases. This result is in excellent agreement with the observations made by Terrones et al. [21].

The relation between the equilibrium spacing between two adjacent shells is shown in Figure 4 for a spherical carbon onion. Using a first order exponential curve fitting technique from Microcal Origin 6.0 and the values of constants provided previously, we may obtain an equation which describes the interspacing between each shell of a spherical carbon onion, namely

$$\text{equilibrium spacing (\AA)} = 3.455 + 0.131e^{-1.593n}, \quad (3.1)$$

where  $n$  is the shell number.

For an ellipsoidal carbon onion, the relation between the spacing number and the equilibrium distance between each layer is shown in Figure 5. Again, using a first order exponential curve fitting technique from Microcal

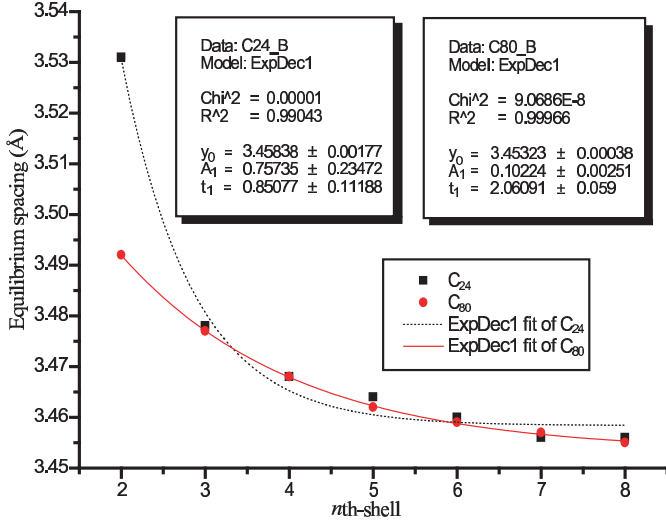


**Fig. 5.** Equilibrium spacing between adjacent shells of spheroidal carbon onions assuming C<sub>24</sub> and C<sub>80</sub> core.

Origin 6.0 and the values of constants provided previously, we obtain respectively the equations which describe the equilibrium spacing between any two neighbouring layers for the C<sub>24</sub> and C<sub>80</sub> ellipsoidal carbon onions, namely

equilibrium spacing

$$\text{for C}_{24} \text{ onion } (\text{\AA}) = 3.458 + 0.757e^{-0.851n},$$

and

equilibrium spacing

$$\text{for C}_{80} \text{ onion } (\text{\AA}) = 3.453 + 0.102e^{-2.061n},$$

where  $n$  is the shell number. We comment from Figure 5 that the large equilibrium spacing between the 1st- and the 2nd-shells of C<sub>24</sub> carbon onion occurs due to the unstable structure of C<sub>24</sub> [11].

## 4 Summary

In this paper, we determine the interspacing between two adjacent layers of spherical and ellipsoidal carbon onions. The Lennard-Jones potential together with the continuum approximation is employed to determine the preferred position or the equilibrium distance for each layer of the carbon onions. The analysis gives rise to the possible dimensions for each shell of the carbon onions. Moreover, we observe that the equilibrium spacing decreases as the shell is further away from the inner core and this is due to the decreasing curvature for the larger spheroids. However, this is not the case when high temperatures and pressures are applied to the onion, as shown by Banhart and Ajayan [22]. Upon heating the particle up to 700 °C and simultaneously irradiating with electrons, the interlayer spacing in the onion is actually shown to decrease from

the outside to the inside, indicating an increasing compressive stress towards the centre which gives rise to a diamond core. Finally, we provide an approximate equation for the determination of the equilibrium spacing for any two adjacent layers of a spherical and an ellipsoidal carbon onion.

The authors are grateful for the Australian Research Council for support through the Discovery Project Scheme and the provision of an Australian Postdoctoral Fellowship for N.T. and an Australian Professorial Fellowship for J.M.H. D.B. is grateful to the Royal Thai Government Scholarship for providing a Ph.D. scholarship.

## Appendix A: Analytical solution for $I_n^*$ in (2.2)

The integral (2.2) may be evaluated either in terms of hypergeometric or Legendre functions. First, we consider the integral

$$I_{2m}^* = \int_0^{2\pi} \int_0^{2\pi} \frac{d\theta_1 d\theta_2}{\{\lambda + \xi \sin^2[(\theta_1 - \theta_2)/2]\}^m}, \quad (\text{A.1})$$

where  $m = n/2$ . Since the integrand is a symmetric function of  $\theta_1 - \theta_2$ , the intermediate integral  $I_{2m}^{**}$  defined by

$$I_{2m}^{**} = \int_0^{2\pi} \frac{d\theta_1}{\{\lambda + \xi \sin^2[(\theta_1 - \theta_2)/2]\}^m},$$

can be shown by differentiation with respect to  $\theta_2$  to be independent of  $\theta_2$ , namely

$$\frac{dI_{2m}^{**}}{d\theta_2} = \int_0^{2\pi} -\frac{\partial}{\partial \theta_1} \left( \frac{1}{\{\lambda + \xi \sin^2[(\theta_1 - \theta_2)/2]\}^m} \right) d\theta_1 = 0.$$

Thus, we may set  $\theta_2$  to be zero and trivially perform the  $\theta_2$  integration so that (A.1) becomes

$$I_{2m}^* = 8\pi \int_0^{\pi/2} \frac{dx}{(\lambda + \xi \sin^2 x)^m},$$

and we may consider the integral  $I_{2m}$  defined by

$$I_{2m} = \int_0^{\pi/2} \frac{dx}{(\lambda + \xi \sin^2 x)^m}. \quad (\text{A.2})$$

Making the substitution  $t = \cot x$  we obtain

$$\begin{aligned} I_{2m} &= \int_0^\infty \frac{(1+t^2)^{m-1}}{(\lambda + \xi + \lambda t^2)^m} dt \\ &= \frac{1}{(\lambda + \xi)^m} \int_0^\infty \frac{(1+t^2)^{m-1}}{(1 + \omega t^2)^m} dt, \end{aligned}$$

where  $\omega = \lambda/(\lambda + \xi)$ . Now, by writing this integral in the form

$$I_{2m} = \frac{1}{(\lambda + \xi)^m} \int_0^\infty \frac{1}{[1 + (1 - \omega)t^2/(1 + t^2)]^m (1 + t^2)},$$

we can make the substitutions

$$z = \frac{t}{(1+t^2)^{1/2}}, \quad t = \frac{z}{(1-z^2)^{1/2}}, \quad dt = \frac{dz}{(1-z^2)^{3/2}},$$

and in the following line we make the substitution  $u = z^2$

$$\begin{aligned} I_{2m} &= \frac{1}{(\lambda + \xi)^m} \int_0^1 \frac{dz}{[1 - (1 - \omega)z^2]^m (1 - z^2)^{1/2}} \\ &= \frac{1}{2(\lambda + \xi)^m} \int_0^1 \frac{u^{-1/2} (1 - u)^{-1/2}}{[1 - (1 - \omega)u]^m} du. \end{aligned}$$

From Gradshteyn and Ryzhik [23] (p. 995, Eq. (9.111)) we may deduce

$$I_{2m} = \frac{\pi}{2(\lambda + \xi)^m} F\left(m, \frac{1}{2}; 1; \frac{\xi}{\lambda + \xi}\right), \quad (\text{A.3})$$

where  $F(a, b; c; z)$  denotes the usual hypergeometric function. We note that Colavecchia et al. [24] examine in some details the numerical evaluation of various hypergeometric functions.

From Erdélyi et al. [25] and on recognizing two of the numbers  $\pm(1 - c)$ ,  $\pm(a - b)$ ,  $\pm(a + b - c)$  are equal to each other, it can be shown that this result admits a quadratic transformation and becomes a Legendre function. Using the transformation

$$F(a, b; 2b; 4z/(1+z)^2) = (1+z)^{2a} F(a, a+1/2-b; b+1/2; z^2),$$

we obtain

$$I_{2m} = \frac{\pi(1+y)^{2m}}{2(\lambda + \xi)^m} F(m, m; 1; y^2),$$

where  $4y/(1+y)^2 = \xi/(\lambda + \xi)$ . Using the definitions from Gradshteyn and Ryzhik [23] (p. 960, Eq. (8.772.3) and p. 998, Eq. (9.131.1))

$$\begin{aligned} P_\nu^\mu(z) &= \frac{1}{\Gamma(1-\mu)} \left(\frac{z-1}{z+1}\right)^{-\mu/2} \left(\frac{z+1}{2}\right)^\nu \\ &\quad \times F\left(-\nu, -\nu - \mu; 1 - \mu; \frac{z-1}{z+1}\right), \end{aligned}$$

and

$$F(a, b; c, z) = (1-z)^{c-a-b} F(c-a, c-b; c; z),$$

where  $P_\nu^\mu(z)$  is a Legendre function of the first kind and in our case  $\mu$  is zero, then we obtain the integral in terms of the Legendre function which is given by

$$I_{2m} = \frac{\pi}{2(\lambda + \xi)^m} \left(\frac{1+y}{1-y}\right)^m P_{m-1}\left(\frac{1+y^2}{1-y^2}\right). \quad (\text{A.4})$$

## Appendix B: Degenerate hypergeometric functions

Details for the degenerate hypergeometric function arising from (A.3) are presented in this appendix. A degenerate hypergeometric function is one which can be written as a finite sum. For convenience, we define

$$J_m = F(m, 1/2; 1; z), \quad (\text{B.1})$$

where  $m$  is a positive integer. Following Erdélyi et al. [25], since  $c - a$  is a negative integer, equation (B.1) becomes a degenerate hypergeometric function (see formula 16, Erdélyi et al. [25], p. 72) with the degenerate solution

$$F(a, b; c; z) = (1-z)^{c-a-b} F(c-a, c-b; c; z).$$

Then we obtain

$$J_m = (1-z)^{1/2-m} F(1-m, 1/2; 1; z). \quad (\text{B.2})$$

In terms of a series, the hypergeometric function is given by

$$F(a, b; c; z) = \sum_{n=0}^{\infty} \frac{(a)_n (b)_n}{n! (c)_n} z^n,$$

where  $(a)_n = \Gamma(a+n)/\Gamma(a) = a(a+1)(a+2)\dots(a+n-1)$  and  $(a)_0 = 1$ . Here, we need to evaluate  $J_3$  and  $J_6$ , and from (B.2) we may deduce

$$\begin{aligned} J_3 &= \frac{1}{(1-z)^{5/2}} \sum_{n=0}^2 \frac{(-2)_n (1/2)_n}{n! (1)_n} z^n \\ &= \frac{1}{(1-z)^{5/2}} \left(1 - z + \frac{3}{8} z^2\right), \\ J_6 &= \frac{1}{(1-z)^{11/2}} \sum_{n=0}^5 \frac{(-5)_n (1/2)_n}{n! (1)_n} z^n \\ &= \frac{1}{(1-z)^{11/2}} \left(1 - \frac{5}{2} z + \frac{15}{4} z^2 - \frac{25}{8} z^3 \right. \\ &\quad \left. + \frac{175}{128} z^4 - \frac{63}{256} z^5\right). \end{aligned} \quad (\text{B.3})$$

## References

1. M.S. Dresselhaus, G. Dresselhaus, P.C. Eklund, *Science of Fullerenes and Carbon Nanotubes* (Academic Press, California, 1995)
2. H. Terrones, M. Terrones, *New J. Phys.* **5**, 126.1 (2003)
3. S. Weber, *Crystallography Picture Book* (<http://www.jcrystal.com/steffenweber/pb/>)
4. Q. Zheng, Q. Jiang, *Phys. Rev. Lett.* **88**, 045503 (2002)
5. Q. Zheng, J.Z. Liu, Q. Jiang, *Phys. Rev. B* **65**, 245409 (2002)
6. H.B. Peng, C.W. Chang, S. Aloni, T.D. Yuzvinsky, A. Zettl, *Phys. Rev. Lett.* **97**, 087203 (2006)
7. Z. Slanina, P. Pulay, S. Nagase, *J. Chem. Theory Comput.* **2**, 782 (2006)

8. O.E. Glukhova, A.I. Zhbanov, A.G. Rezkov, *Phys. Solid State* **47**, 390 (2005)
9. J.P. Lu, W. Yang, *Phys. Rev. B* **49**, 11421 (1994)
10. H. Guérin, *J. Phys. B: At. Mol. Opt. Phys.* **30**, L481 (1997)
11. M. Yoshida, E. Osawa, *Full. Sci. Technol.* **1**, 55 (1993)
12. H. Kitahara, T. Oku, K. Suganuma, *Eur. Phys. J. D* **16**, 361 (2001)
13. I. Narita, T. Oku, K. Suganuma, K. Hiraga, E. Aoyagi, *J. Mater. Chem.* **11**, 1761 (2001)
14. S. Iglesias-Groth, J. Breton, C. Girardet, *Chem. Phys. Lett.* **265**, 351 (1997)
15. L.A. Girifalco, M. Hodak, R.S. Lee, *Phys. Rev. B* **62**, 13104 (2000)
16. M. Rieth, *Nano-Engineering in Science and Technology: An Introduction to the World of Nano-Design* (World Scientific Publishing Co. Pte. Ltd., Singapore, 2003)
17. P.J.F. Harris, *Carbon Nanotubes and Related Structures* (Cambridge University Press, England, 1999)
18. H.W. Kroto, K. McKay, *Nature* **331**, 328 (1988)
19. S. Itoh, P. Ordejón, D.A. Drabold, R.M. Martin, *Phys. Rev. B* **53**, 2132 (1996)
20. B.I. Dunlap, R. Zope, *Efficient quantum-chemical geometry optimization and the structure of large icosahedral fullerenes* (<http://arxiv.org/abs/cond-mat/0603225>)
21. M. Terrones, G. Terrones, H. Terrones, *Struct. Chem.* **13**, 373 (2002)
22. F. Banhart, P.M. Agayan, *Nature* **382**, 433 (1996)
23. I.S. Gradshteyn, I.M. Ryzhik, *Table of Integrals, Series, and Products* (Academic Press, San Diego, 2000)
24. F.D. Colavecchia, G. Gasaneo, J.E. Miraglia, *Comput. Phys. Comm.* **138**, 29 (2001)
25. A. Erdélyi, W. Magnus, F. Oberhettinger, F.G. Tricomi, *Higher Transcendental Functions* (McGraw-Hill, New York, 1953)